SCIENTIFIC REPORTS

OPEN

SUBJECT AREAS:
REPRODUCTIVE BIOLOGY
ORGANELLES

Received
8 October 2014

Accepted
15 December 2014

Published
14 January 2015

Correspondence and requests for materials should be addressed to J.C. (joan.cerda@irta.cat)

Mitochondrial aquaporin-8-mediated hydrogen peroxide transport is essential for teleost spermatozoon motility

François Chauvigné[1,2], Mónica Boj[1], Roderick Nigel Finn[2,3] & Joan Cerdà[1]

[1]Institut de Recerca i Tecnologia Agroalimentàries (IRTA)-Institut de Ciències del Mar, Consejo Superior de Investigaciones Científicas (CSIC), 08003 Barcelona, Spain, [2]Department of Biology, Bergen High Technology Centre, University of Bergen, 5020 Bergen, Norway, [3]Institute of Marine Research, Nordnes, 5817 Bergen, Norway.

Reactive oxygen species (ROS), particularly hydrogen peroxide (H_2O_2), cause oxidative cell damage and inhibit sperm function. In most oviparous fishes that spawn in seawater (SW), spermatozoa may be exposed to harmful ROS loads associated with the hyperosmotic stress of axonemal activation and ATP synthesis from mitochondrial oxidative phosphorylation. However, it is not known how marine spermatozoa can cope with the increased ROS levels to maintain flagellar motility. Here, we show that a marine teleost orthologue of human aquaporin-8, termed Aqp8b, is rapidly phosphorylated and inserted into the inner mitochondrial membrane of SW-activated spermatozoa, where it facilitates H_2O_2 efflux from this compartment. When Aqp8b intracellular trafficking and mitochondrial channel activity are immunologically blocked in activated spermatozoa, ROS levels accumulate in the mitochondria leading to mitochondrial membrane depolarisation, the reduction of ATP production, and the progressive arrest of sperm motility. However, the decreased sperm vitality underlying Aqp8b loss of function is fully reversed in the presence of a mitochondria-targeted antioxidant. These findings reveal a previously unknown detoxification mechanism in spermatozoa under hypertonic conditions, whereby mitochondrial Aqp8b-mediated H_2O_2 efflux permits fuel production and the maintenance of flagellar motility.

Spermatozoon motility is a major physiological determinant of male fertility. Amongst external fertilizers, such as freshwater and marine fishes, activation of motility is respectively induced by the hypo- or hyper-osmotic aquatic environment into which the sperm are ejaculated[1–4]. Spermatozoon flagellar motility is primarily driven by the hydrolysis of ATP, which is synthesised from glycolysis and/or mitochondrial oxidative phosphorylation (OXPHOS) depending on the species[5–9]. Due to electron leakage from the mitochondrial electron transport chain during OXPHOS[10], however, or directly resulting from the osmotic stress of activation[11–15], reactive oxygen species (ROS), such as hydrogen peroxide (H_2O_2), may be produced in excess causing depolarisation of the mitochondrial membrane potential ($\Delta\Psi_m$) and mitochondrial malfunctioning[10,16,17]. As a result, spermatozoa enter into oxidative stress, which may lead to membrane lipid peroxidation, depletion of ATP, or axoneme damage, thus inhibiting sperm motility[18–22].

In marine teleosts, oxidative damage in spermatozoa linked to osmotic stress may be particularly critical since these cells face a strong hyperosmotic shock (from ~300 to ~1100 mOsm) when they are released into seawater (SW). Such osmotically-induced H_2O_2 may subsequently diffuse into the mitochondrion further exacerbating the toxic effects of ROS. As in mammals, however, the normal detoxification pathways involving antioxidants, enzymes and peroxisomes that are present in somatic cells[23], are more limited in spermatozoa[24–26], due in part to the relatively low cytoplasmic volume following spermiogenesis and the transcriptional quiescence of the germ cells[27]. Consequently, it is not known how marine fish spermatozoa maintain motility and thus a fertilisation potential during high endogenous production of ROS.

In recent years, aquaporin homologues from plants and animals that facilitate transmembrane water transport, have also been identified as H_2O_2 channels[28–33]. Amongst these homologues is human aquaporin-8 (AQP8), which also transports ammonia[34], and has been shown to be present in the inner mitochondrial membrane of hepatic[35] and renal proximal tubule cells[36], where it is suggested to mediate ammonia and H_2O_2 transport[37,38] rather than water fluxes[37,39]. However, direct evidence that mitochondrial AQP8 mitigates cellular oxidative stress in a physiological framework has not yet been reported.

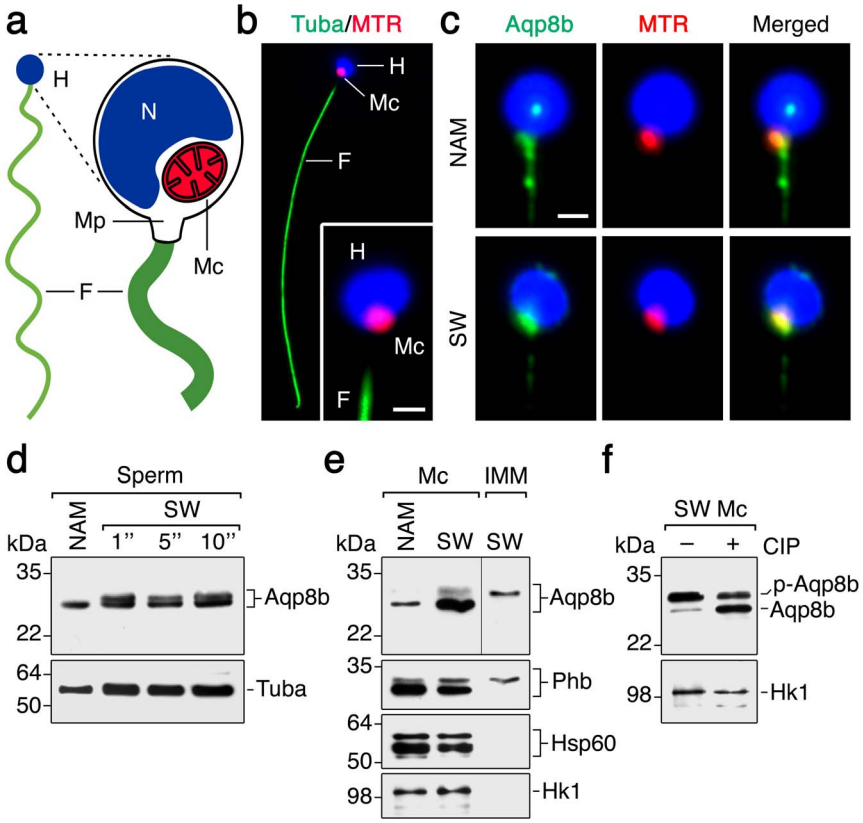

Figure 1 | Aqp8b is phosphorylated and rapidly accumulated in the mitochondrion of the seabream spermatozoa upon SW activation. (a) Schematic diagram of the seabream spermatozoa. (b, c) Immunolocalisation of α-tubulin (Tuba) in immotile spermatozoa (green in b), and Aqp8b (green in c) in non-activated and SW-activated spermatozoa. In (b) and (c), the spermatozoon nucleus and mitochondrion were counterstained with DAPI (blue) and the mitochondrial dye MitoTracker (red), respectively. Scale bars, 1 μm. (d) Representative Western blot of Aqp8b, and Tuba as loading control, in non-activated and activated spermatozoa for 1, 5 or 10 s. (e) Aqp8b immunoblot of mitochondria and mitochondrial inner membrane isolated from immotile and motile spermatozoa. Phb and Hk1 were used as markers of inner and outer mitochondrial membrane, respectively, and Hsp60 as marker of the mitochondrial matrix. (f) Dephosphorylation of mitochondrial Aqp8b by phosphatase treatment. Phosphorylated (p-Aqp8b) and dephosphorylated Aqp8b are indicated. Hk1 was used as loading control. Full-length blots in (d–f) are presented in Supplementary Fig. S3 online. H, head; F, flagellum; Mp, midpiece; N, nucleus; Mc, mitochondria; IMM, inner mitochondrial membrane; CIP, calf intestine alkaline phosphatase; MTR, MitoTracker.

In the oviparous marine teleost, gilthead seabream (*Sparus aurata*), a recent study revealed that upon SW activation of spermatozoa, the teleost orthologue of AQP8, termed Aqp8b, is rapidly accumulated in the single mitochondrion of these cells[40]. In the present work, we therefore selected the seabream as a model to test the hypothesis that H_2O_2 transport through mitochondrial Aqp8b may be essential for the maintenance of motility of marine spermatozoa. Our data show that seabream Aqp8b operates as a mitochondrial peroxiporin in activated sperm and that immunological inhibition of channel function causes mitochondrial failure and the decline of motility, whereas these effects are fully reversed using a mitochondria-targeted antioxidant. These findings uncover a novel aquaporin-mediated detoxification mechanism in spermatozoa and demonstrate a physiological role of mitochondrial AQP8-facilitated H_2O_2 transport.

Results

Seabream Aqp8b is phosphorylated and transported to the spermatozoon mitochondrion upon activation. The mature spermatozoon of seabream is a uniflagellated cell, differentiated into an acrosome-less head, a short midpiece and a long cylindrical flagellum bearing the microtubule-forming axoneme[41] (Fig. 1a). In the midpiece region, a single large mitochondrion is present, which is typical of the spermatozoa of many members of the family Sparidae[41]. Both the flagellum and mitochondrion can be respectively labelled with anti-α-tubulin antibodies and the mitochondria-specific vital dye MitoTracker (Fig. 1b). Immunofluorescence microscopy of ejaculated spermatozoa maintained in non-activating medium (NAM), using the MitoTracker and an affinity-purified antibody against the seabream Aqp8b C-terminus (Aqp8b-Ab)[40], indicated that Aqp8b is located in the midpiece region and anterior part of the flagellum in immotile sperm, whereas the channel accumulates in the mitochondrion upon SW activation (Fig. 1c). Immunoblotting of whole sperm in NAM detected a single reactive band with the expected size of the Aqp8b monomer (28 kDa), while an additional band of slightly higher molecular mass (~30 kDa) was seen already within 1 s of exposure of spermatozoa to SW (Fig. 1d). Subcellular fractionation of spermatozoa and further immunoblotting of Aqp8b together with markers for the inner and outer mitochondrial membrane and mitochondrial matrix, prohibitin (Phb), hexokinase 1 (Hk1) and heat shock protein 60 (Hsp60), respectively, revealed a higher prevalence of both Aqp8b immunoreactive bands in the mitochondrion of activated sperm, thus confirming the immunostaining data, while only a single higher molecular mass band was detected in the inner mitochondrial membrane subcompartment (Fig. 1e). Further treatment of the whole mitochondrial extract from SW spermatozoa with alkaline phosphatase reduced the intensity of the 30-kDa Aqp8b reactive band (Fig. 1f), suggesting that this band most likely corresponds to a phosphorylated form of Aqp8b. These data indicate that Aqp8b is phosphorylated and rapidly trafficked (<1 s) to the inner mitochondrial membrane of the seabream spermatozoon upon SW activation.

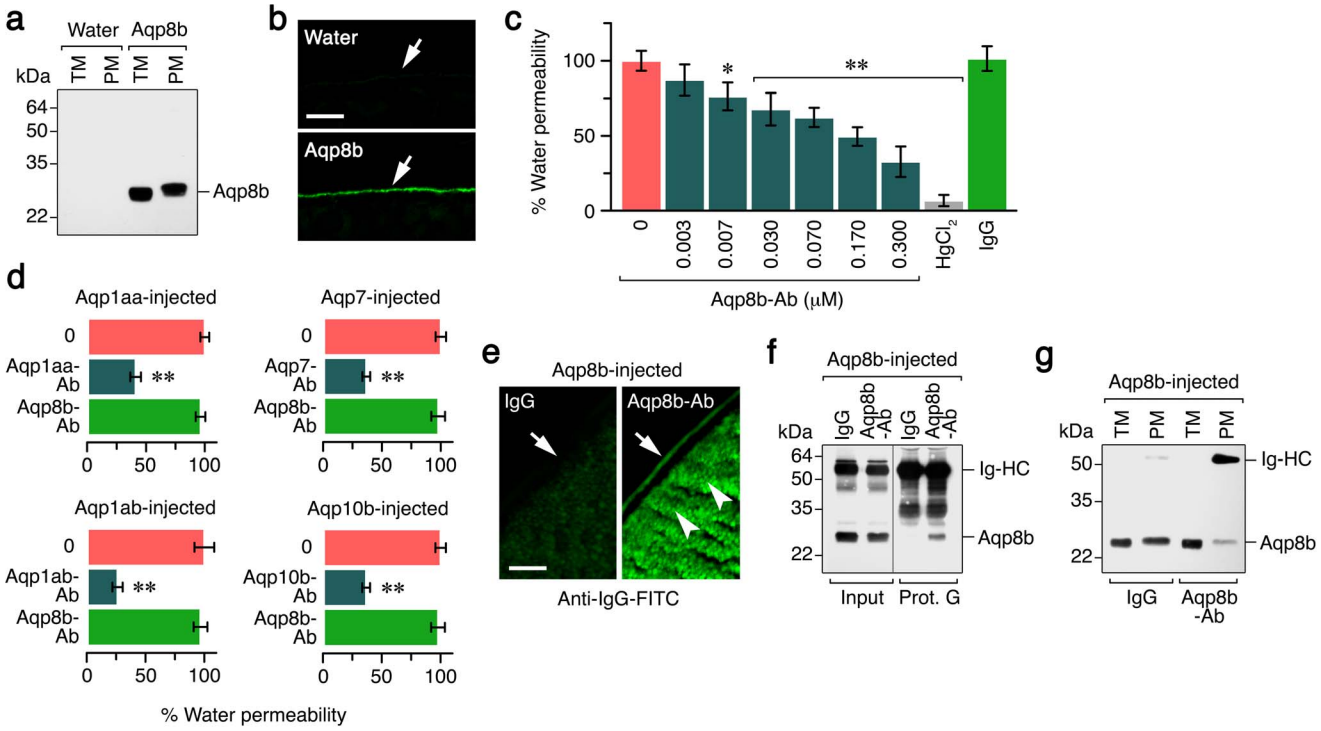

Figure 2 | Specific immunological inhibition of Aqp8b channel function in *X. laevis* oocytes. (a) Western blot of total and plasma membrane (2 oocyte equivalents/lane) of oocytes injected with water (control) or 2 ng Aqp8b cRNA. (b) Immunolocalisation of Aqp8b (green) in water and cRNA-injected oocytes. The arrow points to the plasma membrane labelled for Aqp8b. Scale bar, 20 μm. (c) Percentage of water permeability of Aqp8b oocytes treated with increasing amounts of exogenous Aqp8b-Ab, mercury (100 μM) or IgG (0.3 μM). See Supplementary Fig. S1 online for the original P_f data. (d) Percentage of water permeability of oocytes injected with seabream Aqp1aa, -1ab, -7 or -10b cRNAs (1–5 ng) and exposed to 0.3 μM of the corresponding antibodies or the Aqp8b-Ab. In (c), and (d), data are the mean ± SEM of three independent experiments using different oocyte batches ($n = 12$ oocytes/treatment). $^*P < 0.05$; $^{**}P < 0.01$, with respect to control oocytes not exposed to antibodies, IgG or mercury. (e) Immunodetection of Aqp8b (green) in Aqp8b-expressing oocytes treated with 0.3 μM IgG or Aqp8b-Ab using only fluorescein isothiocyanate-labelled anti-IgG secondary antibodies. The arrow points to the plasma membrane and arrowheads the cytoplasm. Scale bar, 20 μm. (f) Protein G coprecipitation and immunoblot (2 oocyte equivalents/lane) of Aqp8b-Ab-Aqp8b complexes from oocytes treated with 0.3 μM IgG or Aqp8b-Ab. (g) Western blot of total and plasma membrane (2 oocyte equivalents/lane) of Aqp8b oocytes treated as in (e). Full-length blots in (a), (f) and (g) are presented in Supplementary Fig. S4 online. FITC, fluorescein isothiocyanate, TM, total membrane; PM, plasma membrane; Ig-HC, immunoglobulin heavy chain.

Seabream Aqp8b facilitates H_2O_2 uptake in oocytes and sperm mitochondria. Previous studies have shown that the seabream Aqp8b is permeable to water and urea, but not to glycerol[40]. Amino acid alignment of seabream Aqp8b with human AQP8, which has been shown to transport H_2O_2[30,32], revealed that three of the four Aqp8b residues (H72, C208 and R213) in the aromatic arginine region (ar/R) at the extracellular pore mouth that have been suggested to allow the passage of H_2O_2[32] are conserved[40]. To experimentally test whether the seabream Aqp8b can conduct H_2O_2, we used the *Xenopus laevis* oocyte expression system, which yields good expression of the channel at the oocyte plasma membrane (Fig. 2a, b). We first evaluated volumetrically whether the Aqp8b-Ab was able to block Aqp8b-mediated water transport. The osmotic water permeability (P_f) of Aqp8b-expressing oocytes increased by seven-fold with respect to water-injected (control) oocytes, while mercury reduced the P_f by 93 ± 4% (Fig. 2c; Supplementary Fig. S1 online). Interestingly, externally added Aqp8b-Ab in the presence of 0.5% Me_2SO (DMSO) inhibited oocyte water permeability in a dose-dependent manner up to 67 ± 10%, whereas rabbit IgG was ineffective (Fig. 2c; Fig. S1). The effect of the Aqp8b-Ab was specific since the P_f of oocytes expressing Aqp1aa, -1ab, -7 or -10b, also present in the seabream spermatozoa[40], was not affected by the Aqp8b-Ab treatment, whereas the P_f was inhibited (59–74%) when oocytes were exposed to the corresponding antibodies (Fig. 2d). Staining of Aqp8b-expressing oocytes treated with IgG or Aqp8b-Ab using only fluorescein (FITC)-labelled anti-IgG secondary antibodies revealed specific signals in the plasma membrane and the cytoplasm, indicating that exogenously added antibody was able to bind Aqp8b in both compartments (Fig. 2e, right panel). The binding of the antibody was confirmed by protein G coprecipitation experiments, which detected Aqp8b-Ab-Aqp8b complexes only in oocytes expressing Aqp8b and treated with Aqp8b-Ab (Fig. 2f). Immunoblotting of total and plasma membrane fractions of these oocytes also showed lower amounts of Aqp8b in the plasma membrane when compared with those exposed to IgG (Fig. 2g), suggesting that the Aqp8b-Ab partially prevented the insertion of the channel into the oocyte surface.

The uptake of H_2O_2 by control and seabream Aqp8b-expressing oocytes was subsequently determined using the ROS-sensitive, cell-permeable fluorescent dye 5-(and-6)-chloromethyl-2′,7′-dichlorodihydrofluorescein diacetate, acetyl ester (CM-H_2DCFDA), which has previously been employed to evaluate H_2O_2 transport in yeast cells transformed with heterologous aquaporins[28] as well as in AQP3-expressing mice T cells[31]. For these experiments, control and Aqp8b oocytes were loaded with CM-H_2DCFDA and the increase in oocyte fluorescence following exposure to increasing concentrations of external H_2O_2 was determined spectroscopically. Exogenous H_2O_2 supplementation for 30 min significantly increased fluorescence intensity in a dose-response manner in Aqp8b oocytes, the increase being approximately three-fold higher with respect to controls upon addition of 100 μM H_2O_2 (Fig. 3a). The increase in fluorescence of Aqp8b oocytes was significantly reduced by 72 ± 5% and 90 ± 4% by

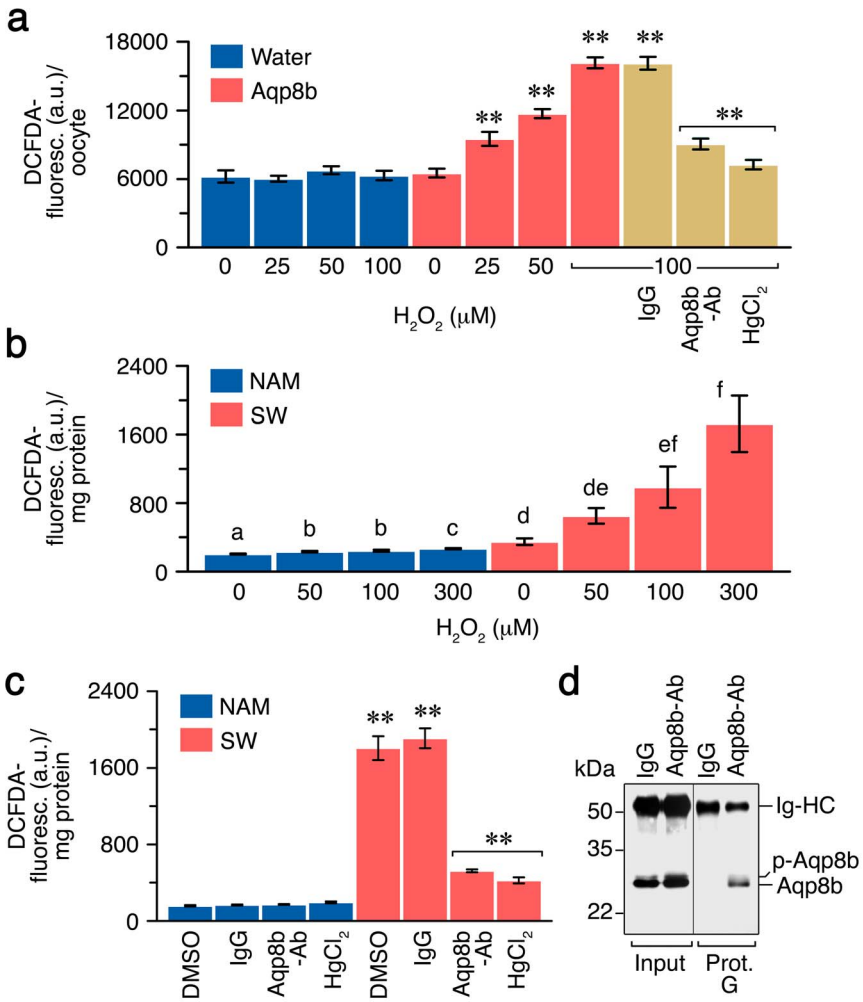

Figure 3 | Seabream Aqp8b facilitates H_2O_2 transport in oocytes and in the mitochondrion of activated spermatozoa. (a) Representative experiment showing H_2O_2 uptake (mean ± SEM, $n = 12$ oocytes) into control and Aqp8b-expressing *X. laevis* oocytes incubated with H_2O_2 determined using the CM-H_2DCFDA reagent. Oocytes exposed to 100 μM H_2O_2 were incubated in the presence or absence of IgG or Aqp8b-Ab (0.3 μM), or $HgCl_2$ (100 μM). (b) Accumulation of H_2O_2 in mitochondria isolated from non-activated and activated spermatozoa and exposed to H_2O_2. Bars with different superscript are significantly ($P < 0.01$) different. (c) H_2O_2 uptake into mitochondria incubated with 300 μM H_2O_2 in the presence or absence of 0.5% DMSO, IgG or Aqp8b-Ab (0.3 μM), or mercury (10 μM). (d) Protein G coprecipitation of Aqp8b-Ab-Aqp8b complexes from mitochondria treated with 0.3 μM IgG or Aqp8b-Ab. In (b) and (c), data are the mean ± SEM ($n = 3$ experiments). In (a) and (c), $*P < 0.05$; $**P < 0.01$, with respect to control oocytes or mitochondria from immotile spermatozoa, or respect to Aqp8b oocytes or SW mitochondria not exposed to the inhibitors (brackets). Full-length blot in (d) is presented in Supplementary Fig. S5 online. Mc, mitochondria; TM, total membrane; PM, plasma membrane; Ig-HC, immunoglobulin heavy chain.

Aqp8b-Ab and $HgCl_2$, respectively, while IgG had no effect (Fig. 3a), suggesting the involvement of Aqp8b in H_2O_2 transport in oocytes.

To corroborate that Aqp8b inserted in the mitochondrion of the seabream spermatozoa was able to facilitate H_2O_2 transport, the uptake of exogenous peroxide by isolated and CM-H_2DCFDA-loaded mitochondria from SW-activated sperm or from immotile sperm maintained in NAM, was estimated as for oocytes. Exogenous peroxide addition resulted in a significant increase of fluorescence intensity of both SW and NAM mitochondria in a dose-response manner, but the increase in fluorescence was much higher in mitochondria from SW-activated sperm (489 ± 18%) compared to mitochondria from NAM spermatozoa (131 ± 2%) (Fig. 3b). Also as observed in oocytes, the fluorescence intensity of SW-activated mitochondria stimulated with 300 μM H_2O_2 was respectively blocked by 78 ± 1% and 84 ± 2% by the Aqp8b-Ab and mercury, and unaffected by the DMSO vehicle or IgG treatment (Fig. 3c). In contrast, the peroxide-induced slight increase in fluorescence of mitochondria from immotile sperm remained unchanged after addition of either of the Aqp8b inhibitors (Fig. 3c). Protein-G precipitation from SW mitochondrial extracts treated with the Aqp8b-Ab pulled down the phosphorylated and dephosphorylated Aqp8b bands, demonstrating the binding of the antibody with endogenous Aqp8b (Fig. 3d). These findings demonstrate that mitochondrial Aqp8b in activated seabream spermatozoa facilitates H_2O_2 transport. In addition, these and previous data indicate that the Aqp8b-Ab can block the trafficking of Aqp8b when heterologously expressed in oocytes, as well as the permeability of the endogenous channel inserted in the spermatozoan inner mitochondrial membrane.

Mitochondrial Aqp8b is required for spermatozoa motility. It has been established that spermatozoa have a limited amount of RNA and are transcriptionally silent[27], although long-lasting mRNA molecules transcribed during spermatogenesis can be translated in spermatozoa by mitochondrial ribosomes[42]. However, in the ejaculated sperm of seabream, *aqp8b* transcripts have not been detected[40]. Therefore, we employed the Aqp8b-Ab to investigate the functional role of Aqp8b during sperm motility in SW. Initial trials indicated that the same concentrations of exogenous antibody

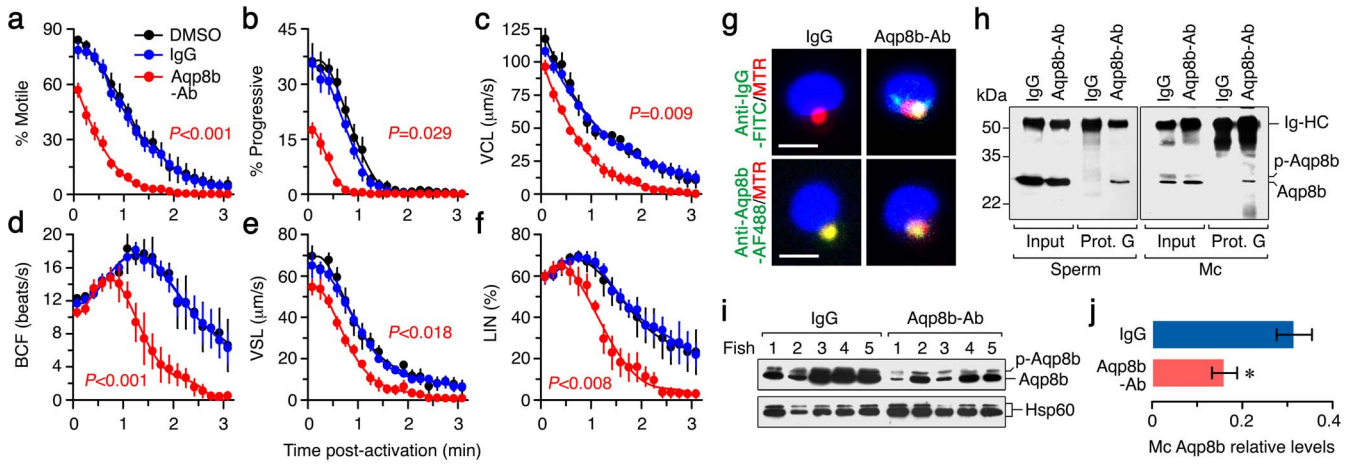

Figure 4 | Mitochondrial Aqp8b is required for spermatozoa motility. (a–f) Kinetic parameters of spermatozoa treated with 0.5% DMSO, in the presence or absence of IgG or Aqp8b-Ab (0.3 μM), after SW activation. Data are the mean ± SEM ($n = 8$ fish). Values of the Aqp8b-Ab-treated groups are significantly different (P indicated in each panel). (g) Merged images of IgG- and Aqp8b-Ab-treated spermatozoa, labelled with MitoTracker (red) and DAPI nuclear stain (blue), which were immunostained (green) with only fluorescein isothiocyanate-labelled anti-IgG or Alexa fluor 488-conjugated Aqp8b-Ab. Scale bars, 2 μm. (h) Protein G coprecipitation of Aqp8b-Ab-Aqp8b complexes in whole sperm and mitochondria from activated spermatozoa treated with 0.3 μM IgG or Aqp8b-Ab. (i) Immunoblot of mitochondrial Aqp8b from SW-activated sperm treated as in (h) using Hsp60 as loading control. In (h) and (i), the immunoglobulin heavy chain (Ig-HC), phosphorylated Aqp8b (p-Aqp8b) and dephosphorylated Aqp8b are indicated. (j) Quantitation (mean ± SEM; $n = 5$ fish) of mitochondrial Aqp8b in (i) normalised to Hsp60, which did not change between treatments ($P = 0.291$). *$P < 0.05$. Full-length blots in (h) and (i) are presented in Supplementary Fig. S6 online. MTR, MitoTracker; Mc, mitochondria; FITC, fluorescein isothiocyanate; AF488, Alexa fluor 488; VCL, curvilinear velocity; BCF, beat cross frequency; VSL, straight-line velocity; LIN, linearity.

tested on oocytes specifically reduced both the percentage of motile and progressive spermatozoa during the 5–10 s interval post-activation in a dose-response manner (Fig. S2). Subsequent time-course experiments up to 3 min revealed that the Aqp8b-Ab drastically reduced the temporal motility (Fig. 4a) and progressivity (Fig. 4b) of activated spermatozoa with respect DMSO- and IgG-treated sperm (controls). In addition, the Aqp8b-Ab affected other kinetic parameters related to the vigour of spermatozoa, such as curvilinear velocity and beat cross frequency (Fig. 4c, d), and progressiveness, such as the straight-line velocity and linearity (Fig. 4e, f).

The staining of spermatozoa treated with IgG or Aqp8b-Ab with MitoTracker and either FITC-labelled anti-IgG or Alexa fluor-labelled Aqp8b-Ab (Fig. 4g), as well as protein G coprecipitation assays of whole sperm and mitochondrial extracts (Fig. 4h), confirmed that the antibody was able to bind extra- and intra-mitochondrial Aqp8b. Further, Aqp8b immunoblotting of mitochondrial extracts from activated spermatozoa showed that the amount of mitochondrial Aqp8b was lower in spermatozoa exposed to the Aqp8b-Ab than in those treated with IgG (Fig. 4i, j), suggesting that the antibody also partially prevented the accumulation of the channel into the mitochondrion.

To investigate the causes for the lower sperm motility found in Aqp8b-Ab-treated spermatozoa, we initially determined the levels of ATP in the whole sperm and mitochondria of spermatozoa exposed to DMSO, IgG or Aqp8b-Ab before and after activation. As expected from studies in other marine fish[3], the total ATP levels in sperm and mitochondria dropped abruptly by 79 ± 2% and 64 ± 5%, respectively, in control sperm at ~1 min post-activation (Fig. 5a). Sperm treated with the Aqp8b-Ab for 1 h in NAM showed the same sperm and mitochondrial ATP levels compared to the control groups, but the decrease of ATP in both sperm (91 ± 2%) and mitochondria (83 ± 2%) of SW-activated spermatozoa was significantly greater than in the DMSO- and IgG-treated sperm (Fig. 5a).

Further, ROS accumulation in spermatozoa was monitored using the CM-H_2DCFDA probe. Spermatozoa loaded with the probe and maintained in NAM did not show detectable levels of fluorescence by microscopy, whereas the compound's fluorescence was strongly and specifically enhanced in the mitochondria within ~10 s of dilution of sperm in SW (Fig. 5b), indicating that this organelle is the major intracellular compartment accumulating ROS upon activation of flagellar motility. Spectroscopic measurement of the intensity of CM-H_2DCFDA fluorescence confirmed the increase of mitochondrial ROS accumulation in control spermatozoa (117 ± 6% and 107 ± 6%, in DMSO and IgG sperm, respectively) (Fig. 5c). However, in Aqp8-Ab-treated sperm the increase in fluorescence was significantly higher (215 ± 13%) (Fig. 5c), suggesting a potential oxidative stress scenario in spermatozoa linked to the inhibition of mitochondrial Aqp8b. Interestingly, evaluation of the $\Delta\Psi_m$ with the lipophilic cationic compound 5,5′,6,6′-tetrachloro-1,1′,3,3′tetraethylbenzymidazolyl carbocyanine iodine (JC-1), which was specific for the sperm mitochondrion (Fig. 5d), revealed that the increase in mitochondrial ROS in DMSO- and IgG-treated sperm during SW activation was not associated with a change in the $\Delta\Psi_m$ (Fig. 5e). In contrast, the JC-1 red:green fluorescence ratio significantly declined by 33 ± 1% in Aqp8b-Ab-treated sperm (Fig. 5e), indicating that the increased accumulation of ROS in the mitochondrion of these spermatozoa led to a decrease of the $\Delta\Psi_m$ and probable mitochondrial damage.

These findings suggested that Aqp8b function in the spermatozoon mitochondrion is necessary to prevent ROS accumulation and depolarisation of the $\Delta\Psi_m$ in order to facilitate ATP production.

Aqp8b functions as a mitochondrial peroxiporin for H_2O_2 efflux during OXPHOS *in vitro*. To investigate further whether Aqp8b can mediate mitochondrial ROS efflux, we measured the production of ATP, the concomitant ROS generation and the variations in the $\Delta\Psi_m$, during OXPHOS *in vitro* by mitochondria isolated from activated sperm. A robust production of ATP was observed after addition of exogenous ADP, that was completely abolished by the ATP synthase inhibitor oligomycin, which confirmed the functionality of the ATP assay (Fig. 6a). The addition of the Aqp8b-Ab however reduced the production of ATP by 38 ± 3%, whereas IgG had no effect (Fig. 6a).

The generation of ROS estimated with the CM-H_2DCFDA dye during ATP production *in vitro*, indicated that DMSO- and IgG-treated mitochondria enhanced both ROS accumulation (by 176 ±

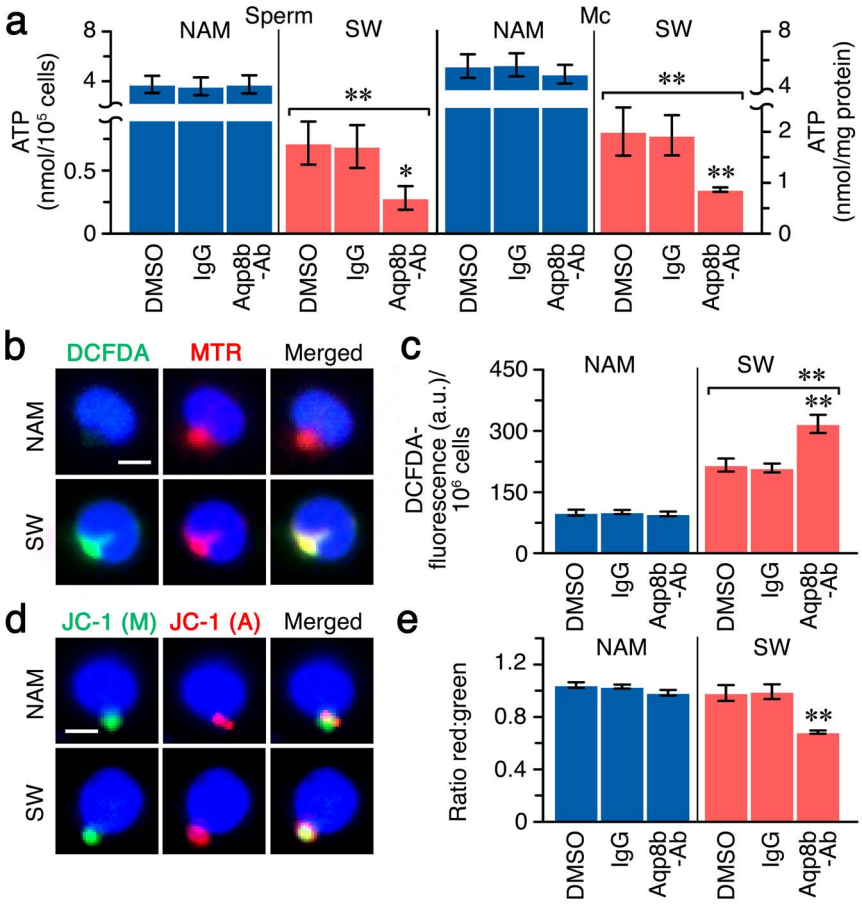

Figure 5 | Inhibition of Aqp8b mitochondrial function increases ROS levels and reduces ATP content in activated spermatozoa. (a) ATP content in spermatozoa and mitochondria before and after activation in SW in the presence of 0.5% DMSO, and 0.3 μM of IgG or Aqp8b-Ab. (b) Epifluorescence photomicrographs of non-activated and activated spermatozoa labelled with the CM-H_2DCFDA dye (green). The nucleus and mitochondrion were counterstained with Hoechst 33342 (blue) and MitoTracker (red), respectively. Scale bar, 1 μm. (c) ROS levels in non-activated and activated spermatozoa treated as in (a) determined using CM-H_2DCFDA. (d) Epifluorescence images of spermatozoa treated as in (b) loaded with the cationic dye JC-1 (green and red) and Hoechst 33342 (blue). Green fluorescence corresponds to JC-1 monomer (M) whereas the formation of red fluorescent J-aggregates (A) is an indicator of the $\Delta\Psi_m$. (e) JC-1 red:green fluorescence intensity ratio of spermatozoa treated as in A. In (a), (c) and (e), data are the mean ± SEM (n = 4–6 fish). *$P < 0.05$; **$P < 0.01$, with respect to spermatozoa in non-activating medium (brackets) or respect to spermatozoa not treated with the Aqp8b-Ab. Mc, mitochondria; MTR, MitoTracker.

15% and 173 ± 20%, respectively) and release (by 220 ± 19% and 221 ± 25%, respectively) (Fig. 6b). In contrast, ROS efflux appeared to be impaired in mitochondria exposed to the Aqp8b-Ab with respect to the controls (147 ± 15%), leading to a higher increase in ROS accumulation (223 ± 10%) (Fig. 6b). Such mitochondrial ROS accumulation was associated with a decrease of the $\Delta\Psi_m$ (by 22 ± 2%) compared to the control groups (Fig. 6c). Addition of the mitochondria-targeted antioxidant mito-TEMPO, which has superoxide and alkyl scavenging properties, reduced the generation of ROS in all treatment groups (Fig. 6b), but interestingly had no effect on the $\Delta\Psi_m$ (Fig. 6c) and the production of ATP (Fig. 6d) in DMSO- and IgG-treated mitochondria. However, in mitochondria treated with the Aqp8b-Ab the antioxidant restored both the $\Delta\Psi_m$ (Fig. 6c) and the production of ATP (Fig. 6d) to control levels.

The antioxidant mito-TEMPO rescues ATP production and motility of Aqp8b-Ab-treated spermatozoa. Treatment with mito-TEMPO completely reversed the Aqp8b-Ab inhibition on mitochondrial ATP production *in vitro*, and we therefore tested further if this antioxidant could prevent the negative actions of Aqp8b-Ab on sperm functions during activation. Consistent with previous results on isolated mitochondria, addition of the antioxidant to IgG-treated spermatozoa was able to reduce the ROS levels (Fig. 7a), but had no effect on the $\Delta\Psi_m$ (Fig. 7b), the ATP content (Fig. 7c), or the different parameters related to spermatozoa motility (Fig. 7d–i). On the contrary, mito-TEMPO-mediated reduction of ROS in Aqp8b-Ab-treated sperm reversed the decrease of the $\Delta\Psi_m$ and ATP content induced by the antibody (Fig. 7a–c), and fully rescued all spermatozoa motility parameters (Fig. 7d–i). These data therefore suggest that the harmful effect on flagellar motility resulting from the inhibition of the Aqp8b function is caused by the accumulation of ROS in the spermatozoa mitochondrion.

Discussion

In this study, we show that mitochondrial Aqp8b plays a vital detoxification role in activated marine teleost spermatozoa. The SW-activated trafficking of Aqp8b to the inner mitochondrial membrane facilitates ROS efflux and thus the maintenance of $\Delta\Psi_m$ and ATP production, which are essential for flagellar motility under hypertonic conditions. Although a previous study has shown H_2O_2 channel activity of mitochondrial AQP8 in human hepatic cultured cells[38], the physiological significance of this mechanism remains unknown. The present study demonstrates the downstream physiological function of an aquaporin orthologue as a mitochondrial peroxiporin.

The expression of aquaporins in seabream spermatozoa, including the water-selective Aqp1aa and -1ab, and water, glycerol and urea-

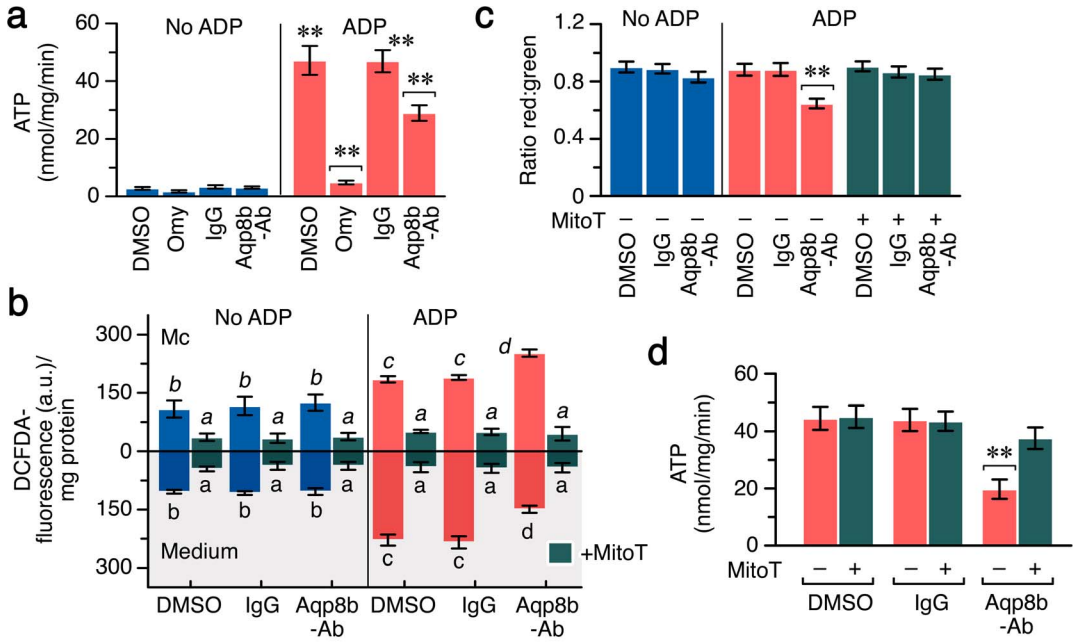

Figure 6 | Mitochondrial Aqp8b mediates ROS release during OXPHOS in vitro. (a) Production of ATP by mitochondria isolated from SW-activated spermatozoa in the presence of absence of ADP (2.5 mM), oligomycin (2 mM), IgG or Aqp8b-Ab (0.3 μM). (b) ROS accumulation and release during ATP production by isolated mitochondria treated as in (a), with or without antioxidant mito-TEMPO (50 μM), determined with CM-H_2DCFDA. (c) JC-1 red:green fluorescence intensity of mitochondria treated as in A during ATP production. (d) Production of ATP in the presence of ADP, with or without addition of mito-TEMPO. Data (mean ± SEM; $n = 3$–4 separate experiments on different fish) in (a), (c) and (d) with asterisks are significantly ($P < 0.01$) different with respect to mitochondria without ADP, or respect to mitochondria treated with ADP and DMSO alone (brackets). In (b), bars with different superscript are significantly different ($P < 0.01$). Omy, oligomycin; MitoT, mito-TEMPO.

transporting Aqp7 and -10b paralogues[40,43], is similar to mammalian sperm where there is convincing evidence for the presence of AQP3, -7, -8 and -11[44,45]. However, although Aqp1ab, -8b and -10b appear to be phosphorylated upon SW activation of seabream spermatozoa[40], only Aqp8b is rapidly (< 1 s) inserted into the inner mitochondrial membrane. The immediacy of Aqp8b accumulation in the mitochondrion is consistent with the extremely fast activation of marine teleost sperm, which is thought to occur in a two-stage process[3]. The first involves water efflux upon contact with the hyperosmotic SW, which rapidly (< 20 ms) creates an expansion of flagellar membranes driving the local activation of strech-activated channels and the stimulation of the axoneme, followed (at ~1 s) by an increase of the internal ionic concentration and ATPase activation[3]. Our data suggest that it is the second event that coincides with the recruitment of Aqp8b in the seabream spermatozoan mitochondrion.

This study thus shows that one of the antioxidant systems present in the seabream spermatozoa, presumably in addition to ROS scavenging enzymes[26,46], is precisely the accumulation of the peroxiporin Aqp8b in the mitochondrion upon SW activation. As in other marine teleosts, most of the energy required for seabream sperm motility is obtained from endogenous ATP stores pre-accumulated during spermatogenesis, as well as produced *de novo* by mitochondrial OXPHOS during the motility phase, rather than glycolysis, which probably plays a minor role during this time[6–8,47]. Additional evidence that supports this model is our finding that mito-TEMPO, which can also inhibit the glycolytic pathway[48], did not affect the ATP content or the motility of activated control spermatozoa. However, OXPHOS-produced ATP also generates ROS as a by-product, which are accumulated in mitochondria possibly together with peroxide generated in the cytoplasm as a result of osmotic stress. Our data in the seabream suggest that to avoid oxidative damage and prolong spermatozoon motility, Aqp8b is specifically delivered to the mitochondrion, where it facilitates the efflux of accumulated H_2O_2. When this pathway is distorted by the alteration of Aqp8b trafficking and/or channel function, increased mitochondrial ROS levels induce the decrease of the $\Delta\Psi_m$ and inhibit the production of ATP, leading to the decline of sperm motility. The existence of this mechanism is further supported by the observation that treatment of immunologically impaired spermatozoa with mito-TEMPO restores the $\Delta\Psi_m$ and the production of ATP, and fully rescues sperm motility.

Marine fish spermatozoa are considered hypermotile, showing a high velocity and a fast consumption of energy, when compared to mammalian spermatozoa, which may be an adaptation to the short period during which the micropyle remains open in fish eggs after contact with SW[3]. However, mammalian spermatozoa acquire a vigorous swimming activity in the vicinity of the ova, the so-called hyperactivation process, which is needed to traverse the zona pellucida and fertilize the egg[49]. Hyperactivation is triggered by a rise in flagellar Ca^{2+} and requires increased pH and ATP production[49]. Therefore, the process of hyperactivation occurring in mammalian spermatozoa under hypotonic conditions is reminiscent of the high motility of marine fish sperm[2,3], and might require the presence of specific mitochondrial detoxification mechanisms. In rodent and human sperm, however, AQP8 is apparently not found in the mitochondria, rather it is specifically localised in the cytoplasmic droplet, where it is suggested to regulate cell volume upon ejaculation in the oviduct[35,44,50]. A potential candidate for mitochondrial peroxide transport might be AQP7, since this aquaglyceroporin can potentially facilitate H_2O_2 transport[32], as shown for AQP3[30,31], and is localised in the mitochondria of human swim-up motile sperm[51]. Thus, the potential role of aquaporins as functional peroxide channels in mammalian spermatozoa, particularly during hyperactivation, is intriguing and merits further investigation.

In summary, the present data provide the first evidence for the physiological role of a mitochondrial aquaporin-mediated ROS-detoxification pathway in male germ cells. This pathway is essential for the prevention of oxidative damage to activated marine teleost spermatozoa, and may have evolved as a selective advantage for

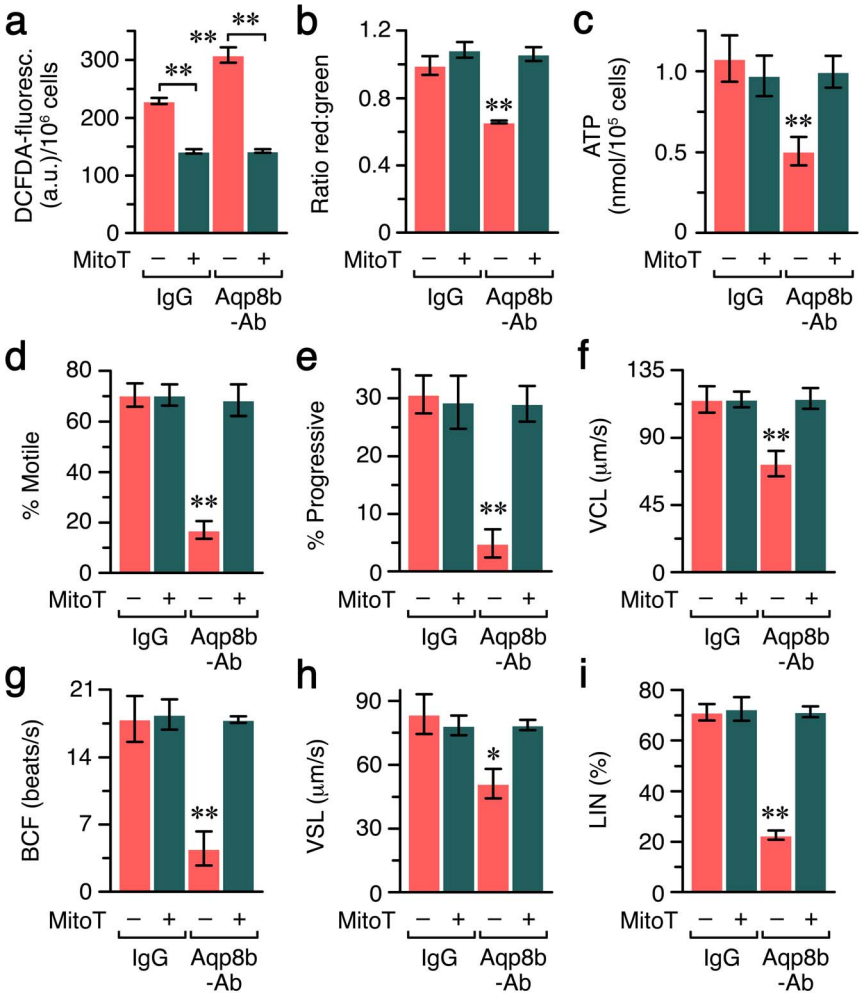

Figure 7 | The mitochondria-targeted antioxidant mito-TEMPO rescues the Aqp8b-Ab-induced decline of sperm motility. (a–c) ROS levels (a), $\Delta\Psi_m$ (b) and ATP content (c) of activated spermatozoa treated with 0.3 μM IgG or Aqp8b-Ab in the presence or absence of 50 μM mito-TEMPO. (d–i) Antioxidant rescue of the Aqp8b-Ab-mediated inhibition of sperm kinetic parameters at 35 s (d-f and h) or 75 s (g and i) post-activation time. Data are the mean ($n = 4$–5 fish). *$P < 0.05$; **$P < 0.01$, with respect to IgG-treated sperm, or as indicated in brackets. MitoT, mito-TEMPO; VCL, curvilinear velocity; BCF, beat cross frequency; VSL, straight-line velocity; LIN, linearity.

increased sperm competition. These results uncover a previously unknown mechanism in sperm physiology and open additional avenues for understanding the impact of oxidative stress on fertilisation.

Methods

Animals and sperm collection. Adult seabream males raised in captivity were maintained as previously described[40]. Milt was recovered from the gonopore of fish sedated with 500 ppm of phenoxyethanol, avoiding SW or urine contamination, stored at 4°C, and used within 24–48 h after collection. Fish samplings were carried out in accordance with the protocols approved by the Ethics Committee of the Institut de Recerca i Tecnologia Agroalimentàries (IRTA, Spain) following the European Union Council Guidelines (86/609/EU).

Fluorescent probes and antibodies. The dyes CM-H_2DCFDA (C6827), JC-1 (T-3168) and MitoTracker® Red CMXRos (M-7512) were from Life Technologies Corp. The Aqp8b-Ab and other affinity-purified antisera against seabream Aqp1aa, -1ab, -7, and -10b have been characterised elsewhere[40,43,52,53]. Antibodies for Hk1, Phb and Hsp60 were from GeneTex (GTX124425, GTX124491 and GTX110039, respectively). Anti-α-tubulin was from Sigma-Aldrich (T9026).

Aquaporin-mediated water and H_2O_2 transport in *X. laevis* oocytes. Ectopic expression of full-length seabream aquaporin cDNAs in oocytes and determination of the P_f was carried out as described previously[40]. For H_2O_2 uptake assays, oocytes were incubated with isotonic modified Bart's solution (MBS; 88 mM NaCl, 1 mM KCl, 2.4 mM $NaHCO_3$, 0.82 mM $MgSO_4$, 0.33 mM $Ca(NO_3)_2$, 0.41 mM $CaCl_2$, 10 mM HEPES, 25 μg/ml gentamycin, pH 7.5) + 0.5% DMSO + 200 μM of CM-H_2DCFDA for 1 h at 18°C. After two washes in MBS, each oocyte was exposed to H_2O_2 (0–100 μM) dissolved in MBS for 30 min at 18°C. Oocytes were washed again and the CM-H_2DCFDA fluorescence of each well (oocyte + MBS) was measured at excitation and emission wavelengths of 495 nm and 525 nm, respectively, using a multiwell plate reader (Infinite M200, Tecan). Data were background corrected to remove non-specific signals of the MBS alone and of oocytes not exposed to the dye. Mercurial inhibition of water and H_2O_2 transport was investigated by incubating oocytes in MBS + 100 μM $HgCl_2$ for 15 min before and during the assays. Aquaporin antibodies and rabbit IgG were tested at 0.003–0.3 μM in the presence of 0.5% DMSO for 1 h before the assays.

Sperm-motility assays. Freshly collected sperm was diluted in NAM (in mg/ml: 3.5 NaCl, 0.11 KCl, 1.23 $MgCl_2$, 0.39 $CaCl_2$, 1.68 $NaHCO_3$, 0.08 glucose, 1 BSA, pH 7.7; 280 mOsm) to 10^9 cells/mL. Sperm motility and different parameters of sperm movement after 1 : 10 dilution in filtered SW for 3 min were determined at room temperature by computer-assisted sperm analysis (CASA) using the Integrated Semen Analysis System software (ISASv1, Proiser) as previously described[40]. For antibody inhibition, immotile sperm was incubated in NAM + 0.5% DMSO + rabbit IgG or the Aqp8b-Ab (0.003–0.3 μM), or with DMSO alone, for 1 h, with or without 50 μM mito-TEMPO (Santa Cruz Biotechnology Inc., sc-221945), before SW activation. Treatments were run in triplicate.

Biochemical fractionation of spermatozoa. Sperm mitochondria were isolated following previous protocols[54,55] slightly modified. Briefly, activated and non-activated sperm (10^9–10^{10} cells/ml) were centrifuged at 1000 × *g* during 1 min and the pellet sonicated for 30 s in 500 μl of the isolation buffer (IB; 0.01 M Tris/Mops pH 7.4, 1 mM EGTA/Tris pH 7.4, 0.25 M sucrose). The cell debris and nuclei were pelleted at 600 × *g* for 10 min at 4°C, and the supernatant centrifuged at 7000 × *g* (10 min, 4°C). The pellet corresponding to the mitochondrial extract was washed once with IB and kept for further experiments. To isolate inner mitochondrial membranes, the mitochondrial pellet was resuspended in 300 μl of 0.3 M sucrose

containing 0.6% digitonin and incubated on ice for 15 min[38]. The extract was diluted 3-fold in 0.3 M sucrose and kept for 15 min on ice before centrifugation at 15000 × *g* (10 min, 4°C). The pellet was resuspended in 300 µl IB, sonicated, diluted with 300 µl of 0.3 M sucrose, and centrifuged as above. The pellet was finally resuspended in 10 ml of 0.3 M sucrose and centrifuged at 100000 × *g* for 1 h, washed, and centrifuged again at 100000 × *g* for 1 h.

Mitochondrial H_2O_2 uptake. Mitochondria were resuspended in 10 ml IB + 0.5% DMSO + 200 µM CM-H_2DCFDA for 1 h, with or without 0.3 µM of IgG or Aqp8b-Ab, or $HgCl_2$ (10 µM; only during the last 15 min), and centrifuged at 7000 × *g* for 5 min at 4°C. Samples were resuspended in equal volumes of fresh IB containing H_2O_2 (0–300 µM) + 0.5% DMSO in the presence of 0.3 µM IgG or Aqp8b-Ab, or $HgCl_2$ (10 µM), as described above. After 30 min, mitochondria were centrifuged, resuspended in fresh IB, and disposed in triplicate in 96-well plates. The fluorescence was measured as indicated previously, and the data were background corrected and normalised to the protein concentration determined by a protein assay.

ATP measurement. ATP content was determined in the whole sperm and mitochondria of non-activated and activated spermatozoa for ~1 min using a bioluminescence ATP determination Kit (Life Technologies Corp., A22066). Sperm and mitochondria were lysed in 50 µl of 2% trichloroacetic acid (TCA) + 2 mM EDTA. After strong vortex, 50 µl of the kit reaction buffer were added to the homogenates. The samples were vortexed again and centrifuged at 14000 × *g* for 5 min at 4°C. Duplicated 10-µl aliquots of the supernatant was used for ATP measurement following the manufacturer's instructions and using a Orion II microplate luminometer (Titertek-Berthold). Data were normalised to the number of cells or the protein content.

Determination of ROS levels in spermatozoa. Sperm in NAM was loaded with 200 µM of the CM-H_2DCFDA dye for 1 h, during which antibodies and drugs were added as described above, centrifuged 1 min at 1000 × *g*, and resuspended in fresh NAM to wash out the dye. Triplicates of 10 µl were loaded in 96-well plates and diluted 1 : 10 in NAM or SW prior to measurement of fluorescence intensity. The background signal of NAM or SW sperm not loaded with the dye was subtracted to each value.

Membrane-potential assays. Sperm samples in NAM were loaded with the JC-1 probe (1 µg/ml) for 30 min, centrifuged and resuspended either in NAM or SW. Fluorescence intensity was measured at an excitation wavelength of 490 nm and emission wavelengths of 535 nm (green) and 595 nm (red), corresponding to the fluorescence peak of the JC-1 monomer (low $\Delta\Psi_m$) and that of the multimeric aggregates (high $\Delta\Psi_m$), respectively. For the calculation of the red:green fluorescence intensity ratio the background fluorescence intensity of samples not incubated with JC-1 was subtracted.

Mitochondrial OXPHOS *in vitro*. Mitochondria isolated from SW spermatozoa were incubated for 1 h in IB containing DMSO, IgG or Aqp8b-Ab, with or without mito-TEMPO (as described above for sperm), or with oligomycin (2 mM) for 10 min. Mitochondria were centrifuged at 7000 × *g* for 5 min, and resuspended in 50 µl fresh IB supplemented with 1 mM pyruvate and 1 mM malate, with or without 2.5 mM ADP for 1 min. Samples were centrifuged at 8000 × *g* for 30 s at 4°C, and the pellet lysed in TCA for ATP measurement. Mitochondrial ROS generation and changes in the $\Delta\Psi_m$ were determined with the CM-H_2DCFDA and JC-1 reagents, respectively, after 1 min of ATP production as previously described. For ROS detection, the fluorescence intensity of the supernatant (ROS released) and of the pellet resuspended in an equal volume of IB (ROS accumulated) were measured separately and normalised to the protein content.

Protein extraction, antibody precipitation and immunoblotting. Total and plasma membrane fractions of *X. laevis* oocytes were isolated as described previously[56]. Sperm, mitochondria and inner mitochondrial membranes were homogenised in 2x Laemmli sample buffer supplemented with protease (EDTA-free Protease Inhibitor Cocktail, Roche) and phosphatase inhibitors (2 mM Na_3VO_4 and 2 mM NaF), and immediately heated at 95°C for 10 min. In some experiments, mitochondria were digested with calf intestine alkaline phosphatase (New England Biolabs Inc.) for 1 h at 37°C prior to Laemmli sample buffer addition. For coprecipitation experiments, samples treated with IgG or Aqp8b-Ab were homogenised in 50 mM Tris-HCl pH 7.4, 150 mM NaCl, 1 mM EDTA, 1 mM EGTA, 5 mM $MgCl_2$, 1 mM NaF, 1 mM Na_3VO_4, 0.5% Triton X-100, and protease inhibitors. After separation of ~10% of the homogenate (input), the rest was mixed with Pure Proteome™ Protein G Magnetic Beads (Merck Millipore) overnight at 4°C, washed three times with PBS + 0.1% Tween-20, and resuspended in Laemmli sample buffer. Protein electrophoresis (12% SDS-PAGE) and immunoblotting was performed as previously described[40]. Primary antibodies were diluted 1 : 1500 (Aqp8b) or 1 : 1000 (Hsp60, Phb and Hk1). For quantitation of mitochondrial Aqp8b abundance normalised to that of Hsp60, the intensity of the immunoreactive bands was determined by densitometry using the Quantity-One software (Bio-Rad Laboratories Inc.).

Fluorescence microscopy. Immunofluorescence microscopy on fixed spermatozoa previously labelled with MitoTracker was carried out as described[40]. Antibodies for Aqp8b and α-tubulin were used at 1 : 600 and 1 : 1000 dilution, respectively. In some experiments, 1 : 100 diluted Aqp8b antibodies labelled with Alexa Fluor 488 using the Zenon® Tricolor Rabbit IgG Labeling Kit #1 (Life Technologies Corp., Z-25360) were used. Live spermatozoa labelled with the nucleic acid stain Hoechst 33342 (Life Technologies Corp., H3570) and MitoTracker together with CM-H_2DCFDA or JC-1 were immobilised on UltraStick/UltraFrost Adhesion slides (Electron Microscopy Sciences). Images were acquired with a Zeiss Axio Imager Z1/ApoTome fluorescence microscope (Carl Zeiss Corp.) using the same fluorescence intensity and exposure for nonactivated and activated spermatozoa.

Statistics. Results are expressed as the means ± SEM. Comparisons between groups were made by the Student *t* test or by one- or two-way ANOVA, followed by Tukey's pairwise comparison. Time-course curves of sperm motility parameters were compared by the Mann-Whitney U test. Statistical analysis were carried out using the Statgraphics Plus 4.1 software (Statistical Graphics Corp.). $P < 0.05$ was considered as statistically significant. For all experiments, sperm samples from at least three different males (one ejaculated per male) were used.

1. Morisawa, M. & Suzuki, K. Osmolality and potassium ion: their roles in initiation of sperm motility in teleosts. *Science* **210**, 1145–1147 (1980).
2. Oda, S. & Morisawa, M. Rises of intracellular Ca^{2+} and pH mediate the initiation of sperm motility by hyperosmolality in marine teleosts. *Cell Mot. Cytoskel.* **25**, 171–178 (1993).
3. Cosson, J. *et al.* Marine fish spermatozoa: racing ephemeral swimmers. *Reproduction* **136**, 277–294 (2008).
4. Vines, C. A. *et al.* Motility initiation in herring sperm is regulated by reverse sodium-calcium exchange. *Proc. Nat. Acad. Sci. USA* **99**, 2026–2031 (2002).
5. Perchec, G., Jeulin, C., Cosson, J., André, F. & Billard, R. Relationship between sperm ATP content and motility of carp spermatozoa. *J. Cell Sci.* **108**, 747–753 (1995).
6. Dreanno, C. *et al.* Effects of osmolality, morphology perturbations and intracellular nucleotide content during the movement of sea bass (*Dicentrarchus labrax*) spermatozoa. *J. Reprod. Fertil.* **116**, 113–125 (1999).
7. Dreanno, C. *et al.* Nucleotide content, oxidative phosphorylation, morphology, and fertilizing capacity of turbot (*Psetta maxima*) spermatozoa during the motility period. *Mol. Reprod. Dev.* **53**, 230–243 (1999).
8. Dreanno, C., Seguin, F., Cosson, J., Suquet, M. & Billard, R. ^{1}H-NMR and ^{31}P-NMR analysis of energy metabolism of quiescent and motile turbot (*Psetta maxima*) spermatozoa. *J. Exp. Zool.* **286**, 513–522 (2000).
9. Piomboni, P., Focarelli, R., Stendardi, A., Ferramosca, A. & Zara, V. The role of mitochondria in energy production for human sperm motility. *Int. J. Androl.* **35**, 109–124 (2012).
10. Collins, Y. *et al.* Mitochondrial redox signalling at a glance. *J. Cell Sci.* **125**, 801–806 (2012).
11. Aitken, R. J., Ryan, A. L., Curry, B. J. & Baker, M. A. Multiple forms of redox activity in populations of human spermatozoa. *Mol. Hum. Reprod.* **9**, 645–661 (2003).
12. Lambert, I. H. Reactive oxygen species regulate swelling-induced taurine efflux in NIH3T3 mouse fibroblasts. *J. Membr. Biol.* **192**, 19–32 (2003).
13. Lambert, I. H., Pedersen, S. F. & Poulsen, K. A. Activation of PLA2 isoforms by cell swelling and ischaemia/hypoxia. *Acta Physiol. (Oxf)* **187**, 75–85 (2006).
14. McCarthy, M. J., Baumber, J., Kass, P. H. & Meyers, S. A. Osmotic stress induces oxidative cell damage to rhesus macaque spermatozoa. *Biol. Reprod.* **82**, 644–651 (2010).
15. Burnaugh, L., Ball, B. A., Sabeur, K., Thomas, A. D. & Meyers, S. A. Osmotic stress stimulates generation of superoxide anion by spermatozoa in horses. *Anim. Reprod. Sci.* **117**, 249–260 (2010).
16. Ortega Ferrusola, C. *et al.* Inhibition of the mitochondrial permeability transition pore reduces "apoptosis like" changes during cryopreservation of stallion spermatozoa. *Theriogenology* **74**, 458–465 (2010).
17. García, B. M. *et al.* The mitochondria of stallion spermatozoa are more sensitive than the plasmalemma to osmotic-induced stress: role of c-Jun N-terminal kinase (JNK) pathway. *J. Androl.* **33**, 105–113 (2012).
18. de Lamirande, E. & Gagnon, C. Reactive oxygen species and human spermatozoa. I. Effects on the motility of intact spermatozoa and on sperm axonemes. *J. Androl.* **13**, 368–378 (1992).
19. de Lamirande, E. & Gagnon, C. Reactive oxygen species and human spermatozoa. II. Depletion of adenosine triphosphate plays an important role in the inhibition of sperm motility. *J. Androl.* **13**, 379–386 (1992).
20. Storey, B. T. Biochemistry of the induction and prevention of lipoperoxidative damage in human spermatozoa. *Mol. Human Reprod.* **3**, 203–213 (1997).
21. Armstrong, J. S. *et al.* Characterization of reactive oxygen species induced effects on human spermatozoa movement and energy metabolism. *Free Radic. Biol. Med.* **26**, 869–680 (1999).
22. Koppers, A. J., De Iuliis, G. N., Finnie, J. M., McLaughlin, E. A. & Aitken, R. J. Significance of mitochondrial reactive oxygen species in the generation of oxidative stress in spermatozoa. *J. Clin. Endocrinol. Metab.* **93**, 3199–3207 (2008).
23. Rocha, M. J., Rocha, E., Resende, A. D. & Lobo-da-Cunha, A. Measurement of peroxisomal enzyme activities in the liver of brown trout (*Salmo trutta*), using spectrophotometric methods. *BMC Biochem* **4**, 2 (2003).
24. Morita, M., Nakajima, A., Takemura, A. & Okuno, M. Involvement of redox- and phosphorylation-dependent pathways in osmotic adaptation in sperm cells of euryhaline tilapia. *J. Exp. Biol.* **214**, 2096–2010 (2011).

25. Hagedorn, M., McCarthy, M., Carter, V. L. & Meyers, S. A. Oxidative stress in zebrafish (*Danio rerio*) sperm. *PLoS One* **7**, e39397 (2012).
26. Martínez-Páramo, S. *et al.* Incorporation of ascorbic acid and α-tocopherol to the extender media to enhance antioxidant system of cryopreserved sea bass sperm. *Theriogenology* **77**, 1129–1136 (2012).
27. Ward, W. S. & Zalensky, A. O. The unique, complex organization of the transcriptionally silent sperm chromatin. *Crit. Rev. Eukaryot. Gene Expr.* **6**, 139–147 (1996).
28. Bienert, G. P. *et al.* Specific aquaporins facilitate the diffusion of hydrogen peroxide across membranes. *J. Biol. Chem.* **282**, 1183–1192 (2007).
29. Dynowski, M., Schaaf, G., Loque, D., Moran, O. & Ludewig, U. Plant plasma membrane water channels conduct the signalling molecule H_2O_2. *Biochem. J.* **414**, 53–61 (2008).
30. Miller, E. W., Dickinson, B. C. & Chang, C. J. Aquaporin-3 mediates hydrogen peroxide uptake to regulate downstream intracellular signaling. *Proc. Natl. Acad. Sci. USA* **107**, 15681–15686 (2010).
31. Hara-Chikuma, M. *et al.* Chemokine-dependent T cell migration requires aquaporin-3-mediated hydrogen peroxide uptake. *J. Exp. Med.* **209**, 1743–1752 (2012).
32. Almasalmeh, A., Krenc, D., Wu, B. & Beitz, E. Structural determinants of the hydrogen peroxide permeability of aquaporins. *FEBS J.* **281**, 647–656 (2014).
33. Vieceli Dalla Sega, F. *et al.* Specific aquaporins facilitate Nox-produced hydrogen peroxide transport through plasma membrane in leukaemia cells. *Biochim. Biophys. Acta* **1843**, 806–814 (2014).
34. Jahn, T. P. *et al.* Aquaporin homologues in plants and mammals transport ammonia. *FEBS Lett.* **574**, 31–36 (2004).
35. Calamita, G. *et al.* The inner mitochondrial membrane has aquaporin-8 water channels and is highly permeable to water. *J. Biol. Chem.* **280**, 17149–17153 (2005).
36. Molinas, S. M., Trumper, L. & Marinelli, R. A. Mitochondrial aquaporin-8 in renal proximal tubule cells: evidence for a role in the response to metabolic acidosis. *Am. J. Physiol. Renal Physiol.* **303**, F458–F466 (2012).
37. Soria, L. R. *et al.* Aquaporin-8-facilitated mitochondrial ammonia transport. *Biochem. Biophys. Res. Commun.* **393**, 217–221(2010).
38. Marchissio, M. J., Francés, D. E., Carnovale, C. E. & Marinelli, R. A. Mitochondrial aquaporin-8 knockdown in human hepatoma HepG2 cells causes ROS-induced mitochondrial depolarization and loss of viability. *Toxicol. Appl. Pharmacol.* **264**, 246–254 (2012).
39. Yang, B., Zhao, D. & Verkman, A. S. Evidence against functionally significant aquaporin expression in mitochondria. *J. Biol. Chem.* **281**, 16202–16206 (2006).
40. Chauvigné, F., Boj, M., Vilella, S., Finn, R. N. & Cerdà, J. Subcellular localization of selectively permeable aquaporins in the male germ line of a marine teleost reveals spatial redistribution in activated spermatozoa. *Biol. Reprod.* **89**, 37 (2013).
41. Maricchiolo, G., Genovese, L., Laurà, R., Micale, V. & Muglia, U. Fine structure of spermatozoa in the gilthead sea bream (*Sparus aurata* Linnaeus, 1758) (Perciformes, Sparidae). *Histol. Histopathol.* **22**, 79–83 (2007).
42. Gur, Y. & Breitbart, H. Mammalian sperm translate nuclear-encoded proteins by mitochondrial-type ribosomes. *Genes Dev.* **20**, 411–416 (2006).
43. Zilli, L. *et al.* Evidence for the involvement of aquaporins in sperm motility activation of the teleost gilthead sea bream (*Sparus aurata*). *Biol. Reprod.* **81**, 880–888 (2009).
44. Yeung, C. H. Aquaporins in spermatozoa and testicular germ cells: identification and potential role. *Asian J. Androl.* **12**, 490–499 (2010).
45. Chen, Q. *et al.* Aquaporin 3 is a sperm water channel essential for postcopulatory sperm osmoadaptation and migration. *Cell Res.* **21**, 922–933 (2011).
46. Chen, Y. K. *et al.* Effect of long-term cryopreservation on physiological characteristics, antioxidant activities and lipid peroxidation of red seabream (*Pagrus major*) sperm. *Cryobiology* **61**, 189–193 (2010).
47. Lahnsteiner, F. & Caberlotto, S. Motility of gilthead seabream *Sparus aurata* spermatozoa and its relation to temperature, energy metabolism and oxidative stress. *Aquaculture* **370–371**, 76–83 (2012).
48. Nazarewicz, R. R. *et al.* Does scavenging of mitochondrial superoxide attenuate cancer prosurvival signaling pathways? *Antioxid. Redox Signal* **19**, 344–349 (2013).
49. Suarez, S. S. Control of hyperactivation in sperm. *Hum. Reprod. Update* **14**, 647–657 (2008).
50. Yeung, C. H., Callies, C., Rojek, A., Nielsen, S. & Cooper, T. G. Aquaporin isoforms involved in physiological volume regulation of murine spermatozoa. *Biol. Reprod.* **80**, 350–357 (2009).
51. Moretti, E., Terzuoli, G., Mazzi, L., Iacoponi, F. & Collodel, G. Immunolocalization of aquaporin 7 in human sperm and its relationship with semen parameters. *Syst. Biol. Reprod. Med.* **58**, 129–135 (2012).
52. Fabra, M., Raldúa, D., Power, D. M., Deen, P. M. & Cerdà, J. Marine fish egg hydration is aquaporin-mediated. *Science* **307**, 545 (2005).
53. Raldúa, D., Otero, D., Fabra, M. & Cerdà, J. Differential localization and regulation of two aquaporin-1 homologs in the intestinal epithelia of the marine teleost *Sparus aurata*. *Am. J. Physiol. Regul. Integr. Comp. Physiol.* **294**, R993–R1003 (2008).
54. Frezza, C., Cipolat, S. & Scorrano, L. Organelle isolation: functional mitochondria from mouse liver, muscle and cultured fibroblasts. *Nat. Protoc.* **2**, 287–295 (2007).
55. McLean, D. J., Korn, N., Perez, B. S. & Thurston, R. J. Isolation and characterization of mitochondria from turkey spermatozoa. *J. Androl.* **14**, 433–438 (1993).
56. Kamsteeg, E. J. & Deen, P. M. Detection of aquaporin-2 in the plasma membranes of oocytes: a novel isolation method with improved yield and purity. *Biochem. Biophys. Res. Commun.* **282**, 683–690 (2001).

Acknowledgments

This work was funded by the Spanish Ministry of Science and Innovation (MICINN; AGL2010-15597 to J.C.), and partially by the Research Council of Norway (178837/40 and 224816/E40 to R.N.F.). M.B. was supported by a predoctoral fellowship (FPI) from Spanish MICINN.

Author contributions

F.C. and J.C. designed research; F.C. and M.B. performed research; R.N.F. contributed new reagents/analytical tools; F.C., M.B. and J.C. analyzed data; and F.C., R.N.F. and J.C. wrote the paper.

Additional information

Supplementary information accompanies this paper at http://www.nature.com/scientificreports

Competing financial interests: The authors declare no competing financial interests.

How to cite this article: Chauvigné, F., Boj, M., Finn, R.N. & Cerdà, J. Mitochondrial aquaporin-8-mediated hydrogen peroxide transport is essential for teleost spermatozoon motility. *Sci. Rep.* 5, 7789; DOI:10.1038/srep07789 (2015).

Supplementary Information

Mitochondrial aquaporin-8-mediated hydrogen peroxide transport is essential for teleost spermatozoon motility

François Chauvigné [1,2], Mónica Boj [1], Roderick Nigel Finn [2,3] & Joan Cerdà [1]

[1]Institut de Recerca i Tecnologia Agroalimentàries (IRTA)-Institut de Ciències del Mar, Consejo Superior de Investigaciones Científicas (CSIC), 08003 Barcelona, Spain; [2]Department of Biology, Bergen High Technology Centre, University of Bergen, 5020 Bergen, Norway; [3]Institute of Marine Research, Nordnes, 5817 Bergen, Norway

Correspondence and requests for materials should be addressed to J.C. (joan.cerda@irta.cat)

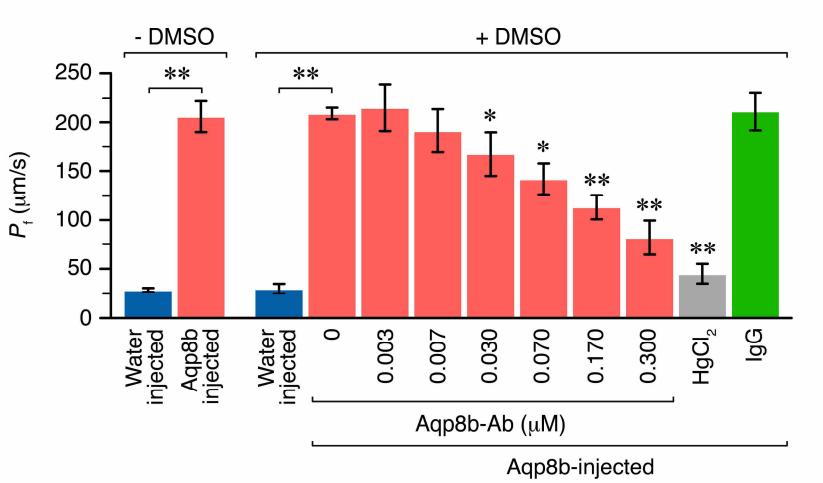

Figure S1 | Specific immunological inhibition of Aqp8b-mediated water transport in *X. laevis* oocytes. Osmotic water permeability (P_f) of water-injected (control) and Aqp8b-expressing oocytes, in the presence or absence of 0.5% DMSO, and increasing amounts of exogenously added Aqp8b antibody (Aqp8b-Ab), 0.3 µM rabbit IgG or 100 µM mercury. Data are the mean ± SEM of three independent experiments using different oocyte batches (n = 12 oocytes/treatment). *P < 0.05; **P < 0.01, with respect to Aqp8b oocytes not exposed to Aqp8b-Ab, or between groups indicated in brackets.

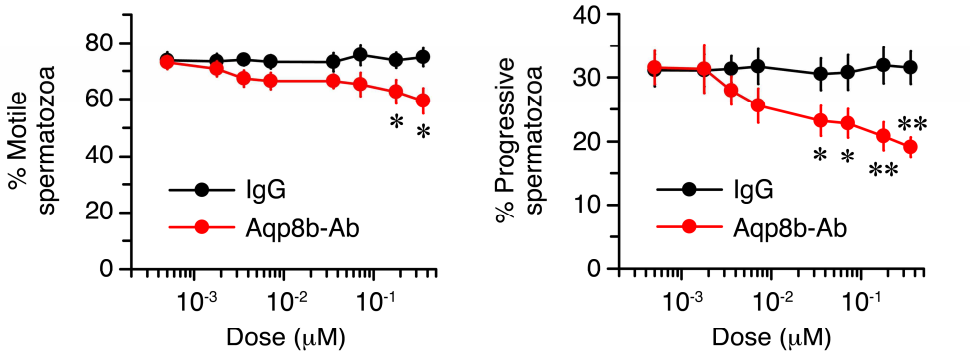

Figure S2 | Effect of increasing doses of IgG or Aqp8b-Ab on seabream spermatozoa motility and progressivity upon activation in SW for 5-10 s. Data are the mean ± SEM (n = 8 fish). *P < 0.05; **P < 0.01, with respect to spermatozoa treated with IgG.

Figure 1d: Aqp8b in sperm

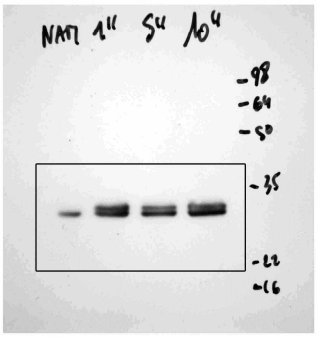

Figure 1d: Tubulin in sperm

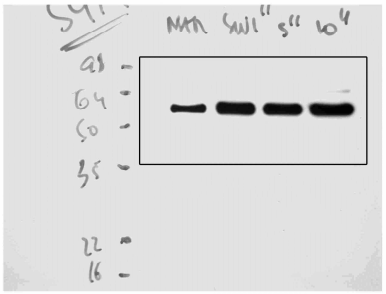

Figure 1e: Aqp8b in Mc and IMM

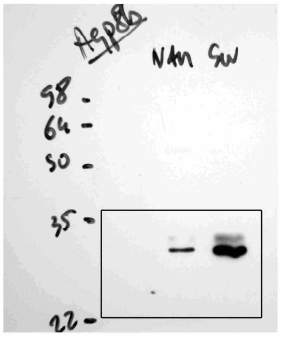

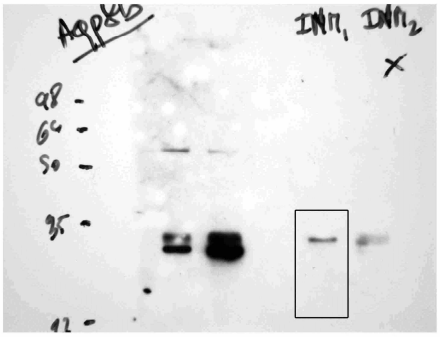

Figure 1e: PhB in Mc and IMM

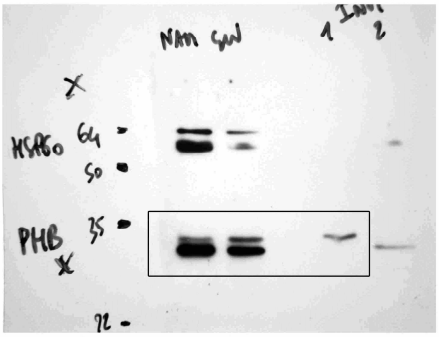

Figure 1e: Hsp60 in Mc and IMM

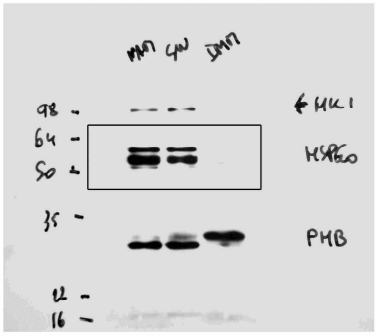

Figure 1e: Hk1 in Mc and IMM

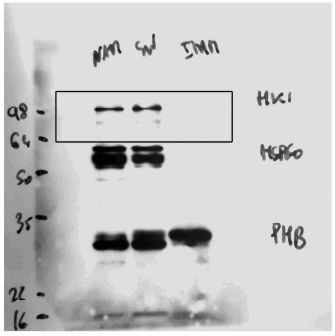

Figure 1f: Aqp8b

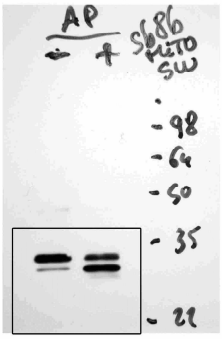

Figure 1f: Hk1

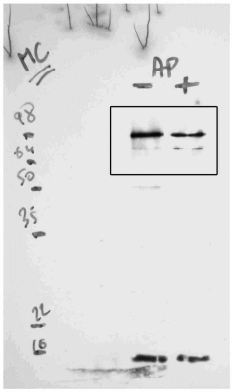

Figure S3 | Full-length blot images for Figure 1. The boxes indicate the part of the blot shown in the main figures.

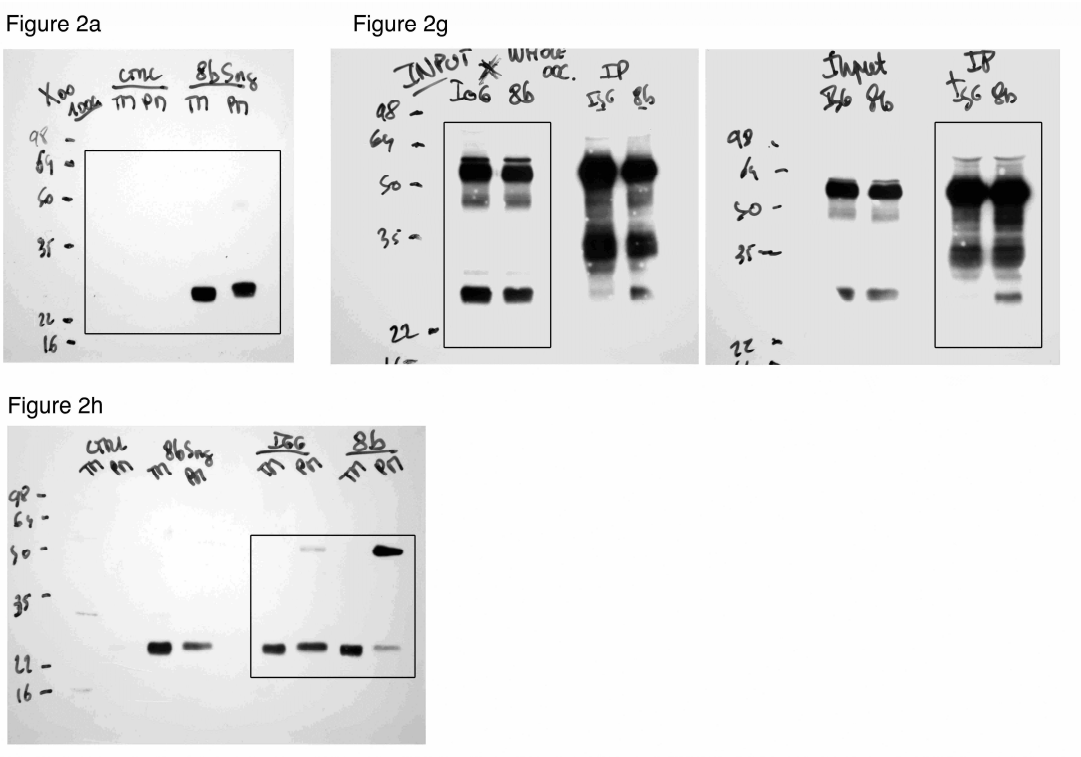

Figure S4 | Full-length blot images for Figure 2. The boxes indicate the part of the blot shown in the main figures.

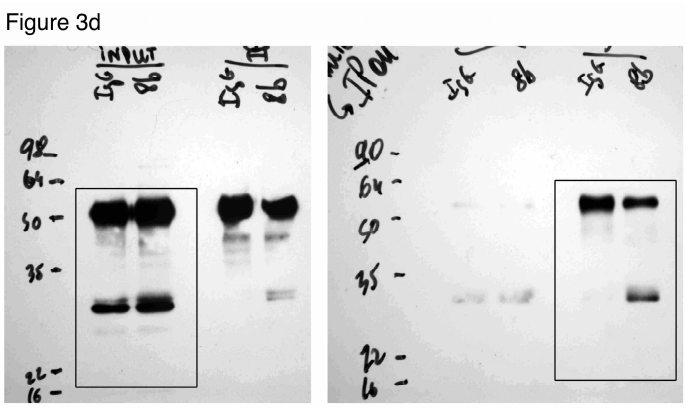

Figure S5 | Full-length blot images for Figure 3. The boxes indicate the part of the blot shown in the main figures.

Figure 4h: sperm

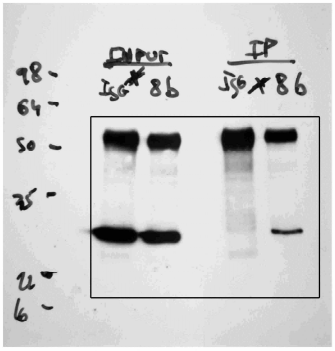

Figure 4h: Mc

Figure 4i: Aqp8b

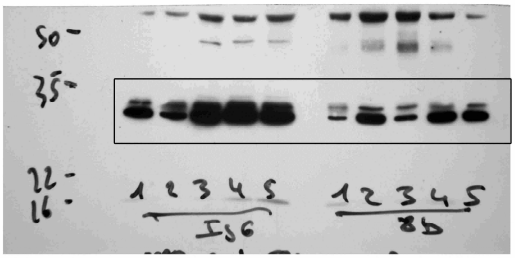

Figure 4i: Hsp60

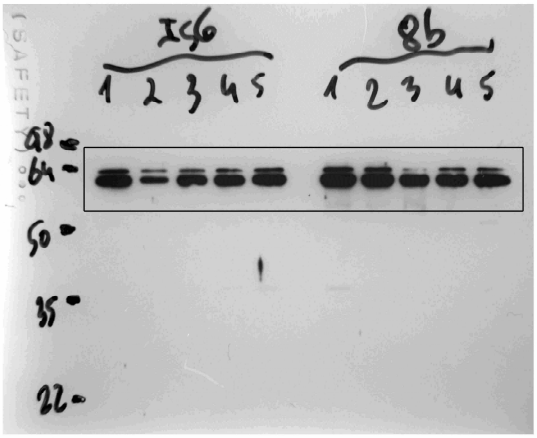

Figure S6 | Full-length blot images for Figure 4. The boxes indicate the part of the blot shown in the main figures. Note than in Figure 4h (Mc blot), the lines IgG and Aqp8b-Ab in the original blot were inverted.